onto the singlet even, singlet odd, triplet even, and triplet odd states, respectively, and

$$V_{SE}=V_{SE}^{C}(r)+U_{SE}(r,p^2),$$
$$V_{SO}=V_{SO}^{C}(r)+U_{SO}(r,p^2),$$
$$V_{TE}=V_{TE}^{C}(r)+U_{TE}(r,p^2)+V_{TE}^{T}S_{12},$$
$$V_{TO}=V_{TO}^{C}(r)+V_{TO}^{LS}\mathbf{l}\cdot\mathbf{S}+V_{TO}^{T}S_{12}.$$

The superscripts C, LS, and T designate the static central, spin-orbit, and tensor parts of the potential. The operators $\mathbf{l}\cdot\mathbf{S}$ and S_{12} are the usual spin-orbit and tensor operators. We have written

$$U_{SE}(r,p^2)=m^{-1}[p^2V_{SE}^{P}(r)+V_{SE}^{P}(r)p^2],$$

U_{SO} and U_{TE} being similarly defined. The symbol m denotes the nucleon mass, r is the relative coordinate $|\mathbf{r}_1-\mathbf{r}_2|$, and p is the relative momentum $\frac{1}{2}|\mathbf{p}_1-\mathbf{p}_2|$. The superscript P indicates that the radial form factor is part of the momentum or velocity-dependent potential.

The radial functions $V^X(r)$ are given by

(i) for $X\neq$P,

$$V^X(r)=-A^X\exp[-(0.6772a^X\mu r)^2]$$
$$-B^X(e^{-\mu r}/\mu r)[1-\exp(-\alpha^X\mu r)],$$

(ii) for $X=$P,

$$V^P(r)=-A^P\exp[-(0.6772a^P\mu r)^2].$$

Here μ is the inverse pion Compton wavelength, $\mu=0.7082$ fm^{-1}.

The parameters of V_{GM} are listed in Table I, and where the parameters differ from those of Green's potential, $V_{SE}(a)+V_{SO}(a)+V_{TE}(a)+V_{TO}(a)$, the parameters of the latter potential are quoted in parentheses. The parameters A^X and B^X for $X\neq$P have the dimensions of energy. The quoted values are in units of fm^{-2}, i.e., they are to be multiplied by $\hbar^2/m=41.469$ MeV fm^2 to convert to MeV. All other parameters are dimensionless.

PHYSICAL REVIEW VOLUME 180, NUMBER 4 20 APRIL 1969

Effect of Woods-Saxon Wave Functions on the Calculation of $A=18$, 206, 210 Spectra with a Realistic Interaction*

S. KAHANA, H. C. LEE,†§ AND C. K. SCOTT‡§
Brookhaven National Laboratory, Upton, New York 11973

(Received 31 December 1968)

The spectra of the nuclei O^{18}, F^{18}, Pb^{206}, Pb^{210} are calculated using realistic forces and a Woods-Saxon form for the shell-model average field. The substitution of Woods-Saxon for harmonic-oscillator single-particle wave functions leads to appreciable upward shifts in the calculated positions for many low-lying levels in the $A=18$ nuclei. In particular the $T=0$, $J=1^+$ and $T=1$, $J=0^+$ binding energies are decreased by 0.6–1.7 MeV. In the heavier nuclei, one finds significant changes in observed energy levels perhaps only for the ground states. Nevertheless, the introduction of the more realistic single-particle average field in the Pb isotopes and in neighboring nuclei permits one to improve the conceptual basis upon which this field is erected.

I. INTRODUCTION

RECENTLY, many authors[1–5] have attempted to derive the residual interaction of the shell model directly from the free nucleon-nucleon force. The spectra obtained with such interactions are invariably calculated using harmonic-oscillator single-particle wave functions. Several authors[6–9] have suggested the changes to be expected if one employs instead the more realistic single-particle Woods-Saxon (WS) wave functions.[10] The present authors deem it necessary to do a somewhat more complete study of the Woods-Saxon shell model. This is especially true in light of our results which indicate that for mass-18 nuclei, the dislocations in level positions resulting from the use of

* Work supported in part by U.S. Atomic Energy Commission.
† Present address: AECL, Chalk River Project, Chalk River, Ontario, Canada.
‡ Present address: Niels Bohr Institute, Copenhagen Ø, Denmark.
§ These authors are grateful to the National Research Council of Canada for continued financial assistance while they were graduate students at McGill University, Montreal, Canada.

[1] J. F. Dawson, I. Talmi, and J. D. Walecka, Ann. Phys. (N.Y.) **18**, 339 (1962).
[2] A. Kallio and K. Kolltveit, Nucl. Phys. **53**, 407 (1964).
[3] S. Kahana and E. Tomusiak, Nucl. Phys. **71**, 402 (1965).
[4] T. T. S. Kuo and G. E. Brown, Phys. Letters **18**, 54 (1965); Nucl. Phys. **85**, 40 (1966).
[5] C. W. Wong, Nucl. Phys. **A91**, 399 (1967).
[6] B. H. Flowers and D. Wilmore, Proc. Roy. Soc. (London) **83**, 683 (1964).
[7] A. P. Stamp and D. F. Mayers, Nucl. Phys. **82**, 296 (1966).
[8] C. W. Wong and C-Y. Wong, Nucl. Phys. **A91**, 433 (1967).
[9] L. A. Sliv and B. A. Volchok, Zh. Eksperim. i Teor. Fiz. **9**, 537 (1959) [English transl.: Soviet Phys.—JETP **36**, 374 (1959)].
[10] R. D. Woods and D. S. Saxon, Phys. Rev. **95**, 577 (1954).

WS functions can be as large as those obtained by adding a core-polarization correction to the interaction.

In this preliminary paper we present the results of a shell-model investigation with WS wave functions in the $A=18$, 206, 210 nuclei. In a later analysis, we will discuss these and other regions of the Periodic Table in more detail. We note here, however, that in Ca^{42} and Sc^{42}, where the individual nucleons are unusually deeply bound, and hence their wave functions are well represented by single oscillator functions, the effect of using a WS average field is minimal. Also we observe perhaps the main lesson to be learned in the Pb^{208} region is that the use of the realistic form for the average field permits one to make a more detailed and intelligent choice of this field. In Sec. II we outline the general approach followed and consider the particular case of the mass-18 nuclei. The Pb nuclei are treated separately in Sec. III.

II. WOODS-SAXON SHELL MODEL FOR O^{18}, F^{18}

A. General Procedure and Choice of Realistic Interaction

The procedure we follow, though leading to lengthy calculation, is quite simple. Our eventual aim is to compute matrix elements of a two-particle residual interaction v_R of the form

$$[(\psi_{n_1l_1j_1}\psi_{n_2l_2j_2})^{JT} \mid v_R \mid (\psi_{n_1'l_1'j_1'}\psi_{n_2'l_2'j_2'})^{JT}]. \quad (1)$$

The WS wave functions involved in this matrix element may be expanded in terms of the oscillator functions $\phi_{nlj}(\mathbf{r})$ in the fashion

$$\psi_{nlj}(\mathbf{r}) = \sum_{n'} a_{nn'(lj)}(\hbar\omega)\phi_{n'(lj)}(\mathbf{r}). \quad (2)$$

It is imperative that for all four WS functions in Eq. (1), we employ a single value of the oscillator parameter $\hbar\omega$. However, we may choose this parameter at our convenience; for example, to minimize the number of terms required in the expansion of Eq. (2). Finally one can exploit the usual machinery of oscillator computations to excute the component calculations implied by Eqs. (1) and (2).

Since we are interested here only in a comparative study of spectra calculated either with oscillator or with WS wave functions, the choice of interaction could perhaps be viewed as secondary. In a phenomenological shell-model calculation, one manufactures an effective force to fit certain aspects of nuclear structure. The use of WS wave functions is then not pertinent. One would simply redetermine the interaction, which could then be said to be wave-function–dependent. Of course, analysis of certain data, such as that obtained from nucleon transfer experiments, might require the use of WS wave functions. If on the other hand, one imagines oneself to be using a so-called "realistic" interaction, it is essential to investigate all avenues which lead to appreciable changes in spectra. For this reason, we employ interactions which have been determined directly from the free-space force as well as one which has been used extensively in phenomenological calculations.

The realistic representation of the residual interaction we use is the free-reaction matrix $K(\epsilon)$, determined directly by the present authors[11] from the free nucleon-nucleon scattering data or derived from a separable potential similar to that introduced by Tabakin.[12] This matrix satisfies the scattering equation

$$K(\epsilon) = v + v[P/(\epsilon - t)]K(\epsilon), \quad (3)$$

where v is the nucleon-nucleon free-space potential, P is a principal value operator, and ϵ is an energylike parameter. The nuclear reaction matrix, which defines the residual interaction in the absence of core polarization, satisfies a similar equation:

$$K_N(E) = v + v[Q/(E - H_0)]K_N(E), \quad (4)$$

where H_0 is the shell-model Hamiltonian, and Q is a projection operator out of the occupied states in the closed shells of the core and out of the valence states.

The selection of H_0, and the concomitant choice of energy E at which $K_N(E)$ is evaluated, is a subject of some controversy. We have,[13] in fact, found from detailed study, that if E is appropriately selected a harmonic-oscillator or core-orthogonalized plane wave description of the intermediate states in Eq. (4) produce very similar results. If the oscillator description is fixed upon, one may take $E=E'+E_{sd}-\Delta$, where $E'\approx -12$ MeV is approximately the ground-state energy of F^{18} or O^{18} relative to the O^{16} core, while $E_{sd}=2(7/2)\hbar\omega$ is the oscillator energy of a pair of nucleons in the $2s$-$1d$ shell. The quantity Δ represents an energy gap between the $2s$-$1d$ valence levels and the unoccupied $2p$-$1f$ shell. To get results in the oscillator case comparable to those obtained using plane wave intermediate states, one should properly employ a state-dependent gap but the choice $\Delta=E_{sd}\approx 94$ MeV for $\hbar\omega=13.4$ MeV is reasonable.

The solution of Eq. (3) may for $\epsilon<0$ be regarded as a reference matrix suitable for a lowest-order approximation to the nuclear reaction matrix. We have suggested using two approaches in evaluating this reference matrix. First, we simply present a parametrized form for $K(\epsilon)$ which is specified by exploiting the relation of its on-the-energy-shell matrix elements to the nucleon-nucleon phase shifts. This phenomenological approach, which we have discussed in detail elsewhere,[11] is clearly a close relative of the phase-shift method.[14] Indeed we

[11] S. Kahana, *Nuclear and Particle Physics* (W. A. Benjamin, Inc., New York, 1968).
[12] F. Tabakin, Ann. Phys. (N.Y.) **30**, 51 (1964).
[13] S. Kahana, H. C. Lee, and C. K. Scott, Phys. Rev. (to be published).
[14] A. Kallio, Phys. Letters **18**, 51 (1965).

TABLE I. Parameters of the phenomenological free-reaction matrix determined by fitting the form presented in Eq. (50) to the Hamada-Johnston phase shifts.

	V_1 (MeV)	V_2 (MeV)	ϵ_0 (MeV)	$\epsilon_1/\lvert\epsilon_0\rvert$	$\epsilon_2/\lvert\epsilon_0\rvert$	μ_1 (fm^{-1})	μ_2 (fm^{-1})
$K(^1S_0)$	−53.8	1221	1.70	4.72	4.40	0.90	3.07
$K(^3S_0)$	−103.3	849	−8.6	1.5	2.28	1.11	2.67

choose ϵ to reflect this relationship. Second, we employ a matrix $K(\epsilon)$ determined from a Tabakin-like separable potential, which has itself been fitted to the scattering data. In this last, more fundamental, approach to the solution of Eq. (3) we select the reference energy ϵ to ensure $K(\epsilon)$ is an accurate first approximation to the nuclear reaction matrix $K_N(E)$.

In the phenomenological free-reaction matrix we permit interaction in only the $^3S_1$ and $^1S_0$ relative states, and take in these states for $\epsilon>0$

$$K(\epsilon)=[(\epsilon+\epsilon_1)/(\epsilon+\epsilon_0)]v_1\exp(-\mu_1 r)+[(\epsilon+\epsilon_2)/(\epsilon+\epsilon_0)][v_2/(mc)^2][p^2\exp(-\mu_2 r)+\exp(-\mu_2 r)p^2], \quad (5)$$

where p^2 is the square of the relative-momentum operator $\mathbf{p}$. A reasonable residual interaction obtains for ϵ in the range 70–100 MeV, and we have settled rather arbitrarily on the value $\epsilon=86$ MeV. We recall that the parameters in Eq. (5) are obtained from a fit to the scattering data. These parameters are given in Table I. The negative value of the parameter ϵ_0 listed for the triplet state indicates the phase shift in this channel becomes $\frac{1}{2}\pi$ for a relative scattering energy $\epsilon=-\epsilon_0$ and ultimately reflects the existence of the deuteron bound state.

TABLE II. Parameters for the separable potential v defined in Eq. (6). These parameters were obtained in a least-squares fit of the Y-IV phase shifts.[a]

$^{2S+1}l_J$	a_1 (fm^{-1})	g_1/a_1 (MeV)	a_2 (fm^{-1})	g_2/a_2 (MeV)
$^3S_1$	1.59	-2.89×10^2	6.23	6.87×10^3
$^3S_1$-$^3D_1$		-7.80×10^1		1.53×10^4
$^3D_1$	1.50	5.44×10^2	6.00	4.86×10^4
$^1P_1$	1.90	4.40×10^2	1.90	4.58×10^5
$^3D_2$	1.29	-2.05×10^2	...	...
$^3D_3$	2.37	-2.56×10^2	...	...
$^1S_0$	1.51	-1.91×10^2	7.29	7.78×10^3
$^3P_0$	1.53	-2.07×10^2	1.53	8.86×10^2
$^3P_1$	1.37	1.14×10^2	1.37	3.11×10^2
$^3P_2$	1.57	-7.38×10^1	1.57	-1.73×10^2
$^1D_2$	1.59	-1.21×10^2	...	...

[a] See Ref. 15.

For our more fundamental determination of $K(\epsilon)$ we employed a two-term factorable potential possessing momentum-space matrix elements

$$(\mathbf{k}\sigma\mid v\mid\mathbf{k}'\sigma')=\sum_{ll'jm}\sum_{i=1}^{2}g_{ll'}{}^{(i)}v_l{}^i(k)v_{l'}{}^i(k')Y_{jls}{}^m(\mathbf{k}\sigma)\times[Y_{jl's}{}^m(\mathbf{k}'\sigma')]^*, \quad (6)$$

where the relative orbital momenta l,l' have been coupled to the two-particle spin S to give a total angular momentum j. In Eq. (6), $\mathbf{k}$ is the relative momentum, σ is a spin label, while $Y_{jls}{}^m(\mathbf{k}\sigma)$ is the conventional spin-orbital function. The sum over i in Eq. (6) extends over two terms; in general, one of these is attractive and the other repulsive. For the s states the analytic form we choose for the attractive form factor

$$v_0{}^1(k)=1/(k^2+a_1{}^2) \quad (7)$$

coincides with that of Tabakin,[10] but the repulsive term which we also take as

$$v_0{}^{(2)}(k)=1/(k^2+a_2{}^2)$$

differs in form from that of Tabakin. Consequently, we obtain a potential possessing a considerably stronger repulsive core than Tabakin's. For the ($^3D_1$) potential form factor we take

$$v_2{}^{1,2}(k)=k^2[k^2+(a_2{}^{1,2})^2]^{-2},$$

while in uncoupled waves for $l>0$ we use

$$v_l{}^i(k)=k^{l+2i-2}[k^2+(a_l{}^i)^2]^{-(i+\frac{1}{2}l)}.$$

The potential parameters for the relative states in which we permitted forces are listed in Table II and Ref. 15. The free-reaction matrix is easily deduced from Eq. (5) by the substitution $g_{ll'}{}^i\delta_{ii'}\to\lambda_{ll'}{}^{ii'}(\epsilon)$, where the functions $\lambda(\epsilon)$ are obtained by appropriate manipulations on Eq. (3). For example, in the ^1S state, $\lambda(\epsilon)$ as a matrix in the indices i and i' satisfies the equation

$$\lambda(\epsilon)=g+g\pi(\epsilon)\lambda(\epsilon), \quad (8)$$

where

$$g=\begin{pmatrix} g^{(1)} & 0 \\ 0 & g^{(2)} \end{pmatrix}$$

and

$$\pi=\begin{pmatrix} \pi^{11} & \pi^{12} \\ \pi^{21} & \pi^{22} \end{pmatrix},$$

[15] R. Seaman, K. A. Friedman, G. Breit, R. D. Haracz, J. M. Holt, and A. Prakash, Phys. Rev. **165**, 1579 (1968).

with

$$\pi^{ii'}(\epsilon)=P\int q^2dq\ v^i(q)v^{i'}(q)\left[\epsilon-\frac{\hbar^2q^2}{m}\right]^{-1}$$

Forces were permitted in all S, P, D relative states. Although tensor coupling was included between the $^3S_1$, $^3D_1$ pair, it appeared to be rather weak for low-energy scattering. We find that our reference matrix $K(\epsilon)$ for $\epsilon=-80$ or -200 MeV reproduces with reasonable accuracy most matrix elements of $K_N(E)$ for the gaps $\Delta=0$, E_{sd}, respectively. We conclude this description of our residual interaction by noting that either version possesses the features one generally associates with the term realistic. In particular, both contain a strong short-ranged repulsion. We believe that effects similar to those presented in the following would result from other realistic interactions.

B. Single-Particle Potential

The WS potential we employ for an average field has the standard form[10]

$$U(r)=U_0(r)+2U_1(r)\mathbf{L}\cdot\mathbf{S},$$

with

$$U_0(r)=-U_0\{1+\exp[(r-R_0)/a]\}^{-1}=-U_0f(r) \quad (9)$$

and

$$U_1(r)=U_{s0}(\hbar/m_\pi c)^2(1/r)\,(d/dr)f(r),$$

where $\mathbf{S}$ is the nucleon spin operator, and m_π the π-meson mass. In fact, we use the conventional value $(\hbar/m_\pi c)^2\approx 2$ fm^2. The parameters in this potential were chosen by fitting the known binding energies of the single-particle $d_{5/2}$, $s_{1/2}$, and $d_{3/2}$ levels in O^{17}. The $d_{3/2}$ level which is unbound by about 1 MeV presents something of a problem. We treated this level by arbitrarily increasing its potential depth and then subtracting the added potential $\Delta U_0(r)$ from the residual interaction. The increment ΔU_0 was varied between 1 and 3 MeV, the former leaving the $d_{3/2}$ level bound by only -0.23 MeV. Little effect was noted in the calculations of two-body matrix elements. To deduce a correct spin-orbit splitting it was necessary to extrapolate the $d_{3/2}$ level into the continuum.

We felt the well radius R_0 would best be determined by following the procedure of Nolen *et al.*[16] for the Ca isotopes. The latter authors suggest one place on the single-particle well the additional restriction that an accurate prediction be obtained for the energy shift between the $d_{5/2}$ ground state of O^{17} and its analog, the ground state of F^{17}. For heavier nuclei one would be in this prescription making rather definite assumptions about the structure of the analog state, but assumptions surely consistent with the shell model. When employing oscillator wave functions, one deduces the parameter $\hbar\omega$ by requiring the matter distribution coincide with the charge distribution determined from electron scattering. For the mass-18 nuclei one thus obtains the standard value $\hbar\omega=13.4$ MeV.

To deduce the Coulomb energy shift discussed above, we have taken the charge distribution in the O^{16} core to be that of a uniformly charged sphere possessing an rms radius $a=2.71$ fm.[17] The resulting Coulomb potential

$$V_c(r)=(Ze^2/2R_u)[3-(r/R_u)^2], \qquad r\leq R_u$$
$$=Ze^2/r, \qquad r>R_u \quad (10)$$

with $R_u=(5/3)^{1/2}a$ the radius of the equivalent charge distribution, is then added to the neutron potential in Eq. (9).

The WS wave functions were calculated using the ABACUS program.[18] In Table III we present the WS potential parametrization obtained and some description of the resulting wave functions. The value of $\hbar\omega$ which maximizes the overlap of a WS function with its main oscillator component[9] is indicated for each level as are the amplitudes of some of the leading terms in the expansion of Eq. (2). Had we plotted the WS wave func-

TABLE III. WS wave functions obtained for the O^{17} valence levels by fitting the absolute positions of the $d_{5/2}$, $s_{1/2}$, and $d_{3/2}$ levels in O^{17} and of the $d_{5/2}$ level in F^{17}. The WS parameters of Eq. (5) are $V_0=57.0$ MeV, $V_{s0}=5.7$ MeV, $a=0.63$ fm, and $r_0=1.17$ fm, where $R_0=r_0A^{1/3}$. The $d_{3/2}$ level is presented for a potential increment $\Delta U_0=1$ MeV. Also shown are the level Coulomb shifts in F^{17} as well as the average r^2 value for the neutron levels. $(\hbar\omega)_{\max}$ is the oscillator parameter which maximizes (Ref. 9) the WS overlap with its main oscillator component. The explicit expansion of each level into single-particle oscillator components is given for the first seven terms.

		$1d_{5/2}$	$2s_{1/2}$	$1d_{3/2}$
E_{nl}(O^{17}) (MeV)	Calculated	−4.106	−3.268	−0.227
	Expt	−4.14	−3.27	0.94
E_C (MeV)	Calculated	3.51	3.14	
	Expt	3.54	3.17	
$\langle r^2\rangle$(fm^2)		11.618	17.79	16.904
$(\hbar\omega)_{\max}$ (MeV)		13.5	12.0	11.0
Oscillator amplitudes				
n				
0		0.988	−0.143	0.958
1		−0.014	0.947	0.001
2		0.137	−0.087	0.234
3		−0.053	0.228	−0.067
4		0.032	0.098	0.091
5		−0.029	0.008	−0.077
6		0.014	−0.072	0.060

[16] J. A. Nolen, Jr., J. P. Schiffer, N. Williams, and D. Von Ehrenstein, Phys. Rev. Letters **18**, 1140 (1967).

[17] H. R. Collard, L. R. B. Elton, and R. Hofstadter, in *Nuclear Radii*, edited by H. Schopper (Landolt-Bornstein, Springer-Verlag, Berlin, 1967), Group 1, Vol. 2.

[18] E. H. Auerbach, BNL Report No. 6562 (unpublished).

TABLE IV. Spectra obtained for the $A=18$ nuclei using WS wave functions and the phenomenological free reaction matrix $K(\epsilon)$ for $\epsilon=86$ as a residual interaction. Only the s-wave parts of the reaction matrix, as shown in Eq. (5) are included. The oscillator spectra for $\hbar\omega=13.4$ and 12 MeV are presented for comparison. All energies are in MeV.

Level	Oscillator $\hbar\omega=13.4$	Oscillator $\hbar\omega=12$	WS
$T=0, J^\pi=1^+$	−5.05	−4.80	−3.98
3^+	−3.97	−3.68	−3.37
5^+	−4.06	−3.78	−3.90
2^+	−1.67	−1.43	−1.06
1^+	1.05	−0.95	−0.12
3^+	−0.32	−0.28	−0.20
$T=1, J^\pi=0^+$	−3.05	−2.91	−2.63
2^+	−1.59	−1.43	−1.33
4^+	−0.82	−0.73	−0.73
0^+	0.06	0.12	0.67
2^+	0.15	0.18	0.23

tions, their most prominent feature would be the extent to which the $1d_{3/2}$ and especially the $2s_{1/2}$ functions protrude beyond their oscillator counterparts. We have illustrated this point by including in Table III the square of the average radii for each level.

C. Matrix Elements and Spectra

Finally, we consider the residual interaction matrix elements obtained with WS wave functions. If one uses as a yardstick, the matrix elements calculated with oscillator functions for $\hbar\omega=13.4$ MeV, then one finds all WS matrix elements are reduced in magnitude. The amount of this reduction varies from as little as 10% for a matrix element involving four $d_{5/2}$ wave functions to as much as 50% for a purely $s_{1/2}$ matrix element. Some of this quenching of the force can be obtained by considering, in Table III, the amplitude of the main oscillator components in the WS functions. However, other terms in the expansion are of importance. The physical reason for the reduction is simply the degree to which the cutoff WS potential allows wave functions to spread out in space. The full extension of the wave functions is not described adequately by a single-oscillator component. For example, if one calculated the $(s_{1/2}^4)$, $T=0$, $J=1^+$ matrix element using just the largest oscillator component in Table III, only a 22% reduction in size would result. In all matrix elements calculated in this section, proton wave functions derived from only the nuclear potential were employed. Had we used the proper Coulomb wave functions, the observed quenching would have been even greater.

The $A=18$ spectra calculated both from WS wave functions and from oscillator functions for $\hbar\omega=13.4$ and 12 MeV are shown in Tables IV and V and in Figs. 1 and 2. The residual interactions employed were the phenomenological free-reaction matrix $K(\epsilon)$ for $\epsilon=86$ MeV and the more fundamental free-reaction matrix for $\epsilon=-200$ MeV, respectively. The latter choice was made to ensure our fundamental interaction was reasonably closely matched to that of Wong[5] or of Kuo and Brown.[4] The latter authors use plane-wave intermediate states in solving Eq. (4). The maximum effects relative to the $\hbar\omega=13.4$ oscillator spectrum are seen for the $T=0$, $J=1^+$ or $T=1$, $J=0^+$ levels. The displacement produced in the ground state of F^{18} was large indeed, some 2 MeV, when the more fundamental

TABLE V. Spectra obtained for the $A=18$ nuclei using WS wave functions and as a residual interaction the solution $K(\epsilon)$ of Eq. (3) for the potential of Eq. (6) with $\epsilon=-200$ MeV. The experimental spectrum and spectra calculated using harmonic-oscillator wave functions with $\hbar\omega=13.4$ and 12 MeV are presented for comparison. All energies are in MeV.

Level	Experiment	WS	Harmonic oscillator (i) $\hbar\omega=13.4$	Harmonic oscillator (ii) $\hbar\omega=12$
$T=0, J^\pi=1^+$	−5.01	−3.81	−5.84	−5.21
3^+	−4.07	−3.18	−4.21	−3.66
5^+	−3.88	−3.50	−4.02	−3.53
2^+	−2.49	−1.29	−2.67	−2.00
1^+		0.02	−1.67	−1.37
$3^+(2^+)$	−1.65	−0.29	−0.48	−0.37
$T=1, J^\pi=0^+$	−3.90	−2.05	−2.87	−2.41
2^+	−1.92	−1.35	−1.78	−1.53
4^+	−0.35	−0.58	−0.74	−0.63
0^+	−0.27	0.80	−0.24	−0.10
2^+	0.02	0.09	−0.10	−0.02
3^+	1.47	0.63	0.55	

free-reaction matrix was used. When we employed a purely s-state force with a repulsive component, this shift was just over 1 MeV. As oscillator components of higher n are included in the WS calculation, other partial waves, especially the $^3P_1$ and $^1P_1$ waves in which the potential is known to be strongly repulsive at high energies, play an increasingly important role.

If one uses for comparison purposes the oscillator spectrum calculated with a value of $\hbar\omega\sim 12$ MeV, arrived at by roughly averaging over the oscillator energy parameters which best describe the three valence states, the discrepancies between oscillator and WS spectra are somewhat less. No purely oscillator calculation, however, can reproduce all of the changes wrought by introducing WS wave functions. Our calculations perhaps, indicate the need for a more intelligent choice of $\hbar\omega$, a choice more consistent with the spatial extent of the valence orbits than is the value $\hbar\omega=13\sim 14$ MeV commonly employed with realistic forces. This lesson is of equal importance in other regions of the Periodic Table.

Indeed in hole-hole calculations in N^{14} we find that a reasonable one-oscillator function description of the single-particle states obtains for $\hbar\omega=16$ MeV. The WS well appropriate for the $p_{1/2}$ and $p_{3/2}$ holes is deeper than the corresponding well for particles. In the region of Pb^{208} we shall see that this situation between particles and holes is reversed. It is evident that in N^{14} the use of our prescription for determining the single-particle potential would lead to greater binding energies than those obtained with an oscillator calculation for $\hbar\omega=$ 13.4 MeV. This behavior of hole-hole states relative to particle-particle states had previously been commented on by Wong and Wong.[8]

A computational point worthy of note concerns the advisability of limiting the number of components which enter into the calculation of WS matrix elements. One must certainly truncate the expansion in Eq. (2). We have for the programs involving pure s-wave forces included as many as ten oscillator components to describe the O^{17} valence wave functions. Also for these simpler situations we retained in the matrix elements terms of all orders, up to quartic, in the small amplitudes displayed in Table III. For the more fundamentally derived free-reaction matrix, which contains forces in relative S, P, and D waves, it is tempting to ignore all but terms linear in the small oscillator amplitudes. This can be somewhat inaccurate for a matrix element involving, say, four $2s_{1/2}$ wave functions. If, for example, one were using a very long-ranged force, this matrix element becomes more or less proportional to a product of normalization integrals. Only some 78% of this normalization resides in the single term containing the large $n=1$ oscillator component. A major portion of the missing normalization strength is to be located not in the linear terms, which are clearly off-diagonal in the oscillator radial quantum number, but rather in the terms quadratic in small amplitudes. For matrix elements which vanish in the limit of an infinite-range force or obtained using short-range forces, the situation is not so dramatic.

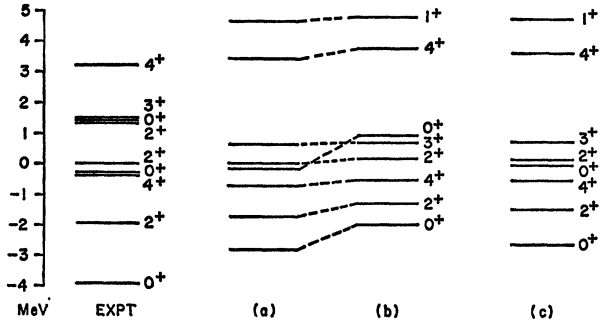

FIG. 1. $T=1$ two-particle spectrum of O^{18} calculated with harmonic oscillator (HO) or Woods-Saxon (WS) wave functions and the fundamental free reaction matrix as a residual interaction. The calculations are for (a) HO, $\hbar\omega=13.4$ MeV, $\epsilon=-200$ MeV; (b) WS, $\epsilon=-200$ MeV; (c) HO, $\hbar\omega=12.0$ MeV, $\epsilon=-200$ MeV.

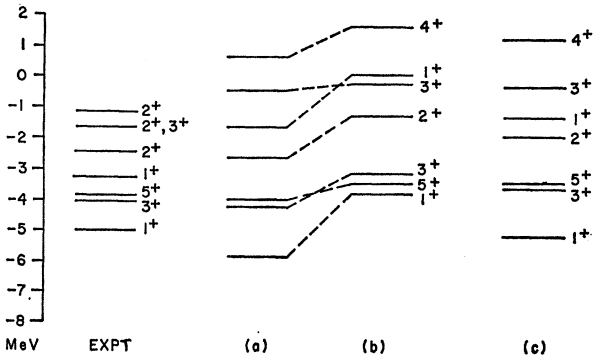

FIG. 2. $T=0$ two-particle states in F^{18} calculated with harmonic oscillator (HO) or Woods-Saxon (WS) wave functions and the fundamental free reaction matrix as a residual interaction. The calculated spectra are (a) HO, $\hbar\omega=13.4$ MeV, $\epsilon=-200$ MeV; (b) WS, $\epsilon=-200$ MeV; (c) HO, $\hbar\omega=12.0$ MeV, $\epsilon=-200$ MeV.

For the spectra obtained using the more fundamental $K(\epsilon)$ and presented in Table V we have used the linear approximation. The matrix elements expected to be sensitive to this approximation were recalculated using the quadratic terms in addition. We found, in particular, that the $T=0$, $J=1^+(s_{1/2})^4$ matrix element was altered from -1.93 to -2.15 MeV while the corresponding $T=1$, $J=0^+$ matrix element changed from -1.14 to -1.29 MeV, in the presence of the quadratic terms. Consequently, the binding energies of the lowest $T=1$, $J=0^+$ or $T=0$, $J=1^+$ states increased by 0.12 and 0.25 MeV, respectively. Energies for states of higher angular momentum are considerably less effected. The disparity indicated in Table V between the harmonic-oscillator $\hbar\omega=13.4$ MeV spectrum and the WS spectrum is thus lessened.

We have further tested the sensitivity of our results to the nature of the force by employing in place of

$K(\epsilon)$ the Rosenfeld mixture[19]

$$v_R(r_{12}) = v_0 \exp(-r_{12}/a)\,(r_{12}/a)^{-1}(0.3+0.7\vec{\sigma}_1\cdot\vec{\sigma}_2)\vec{\tau}_1\cdot\vec{\tau}_2 \tag{11}$$

for the two parametrizations

$$v_0 = -50\text{MeV}, \qquad a = 1.36 \text{ fm}$$

and

$$v_0 = -12\text{MeV}, \qquad a = 2.72 \text{ fm}.$$

We found, for this force, differences between the oscillator and WS spectra very similar to those described above. We used only the s-wave part of the Rosenfeld force and consequently the maximum oscillator-WS shift observed was $\sim$1 MeV for the $T=0$, $J=1^+$ states. One of the criticisms that can be brought against our fundamental realistic interaction $K(\epsilon)$ is the rather short range of the underlying separable potential. We conclude from the Rosenfeld-mixture spectra that although the WS quenching is not too dependent on range, one may be slightly over-estimating the reduction in matrix elements by using $K(\epsilon)$ as a residual interaction.

In concluding this section, we may reiterate a statement made in Sec. I. For light nuclei, one can expect the use of realistic single-particle wave functions to produce level shifts comparable to those which were obtained in the core-polarization calculations of Kuo and Brown.[4] The realistic force we have employed is not unlike that of the latter authors or of Wong.[5] The low-lying $T=0$, $J=1^+$ and $T=1$, $J=0^+$ states were found to be most effected by the change in wave functions. The fits to the experimental 0^+ levels presented by Kuo and Brown for the 0^+ states in O^{18} were perhaps uncomfortably good. From $E2$ transition probabilities observed in this nucleus one expects these states to have a partially deformed character.[20] The weakening of the residual force by the WS wave functions now permits the collective components to play some role in determining the energies of low-lying states.

The use of WS single-particle wave functions leads to some changes in these $E2$ transition probabilities. If we label the states of O^{18} in the transparent fashion 0_1^+, 2_1^+, 0_2^+, etc., then the interesting transitions are $E2(0_2^+\to 2_1^+)$ and $E2(2_1^+\to 0_1^+)$. The use of WS wave functions allows one at a first stage to fit the quadrupole moment of the O^{17} $d_{5/2}$ ground state and the $s_{1/2}\to d_{5/2}$ reduced transition strength with effective charges which differ by only 4%. A reasonable common value for this charge is $e_{\text{eff}}=0.4e$. If one employs oscillator single-particle functions and $\hbar\omega=13.4$ MeV, one requires an effective charge $e_{\text{eff}}=0.52e$ to fit the transition probability but a reduced value $0.42e$ to fit the static moment. With WS two-particle wave functions obtained by diagonalizing our phenomenological free-reaction matrix, the strength of the transition $0_2^+\to 2_1^+$ is increased by a factor of 2.5 over the value obtained from corresponding oscillator functions. The final calculated strength, or $BE(2)$, is still an order of magnitude less than the experimentally observed value 2.22 e^2 fm^4. This effect of the WS functions is at least in part attributable to the weakening of the interaction between the lowest two 0^+ levels. A smaller mixing between the $(s_{1/2}^2)$ and $(d_{5/2}^2)$ configurations in these and the 2_1^+ levels considerably reduces the degree of cancellation in the $0_2^+\to 2_1^+$ transition. At the same time the $2_1^+\to 0_1^+$ transition is slightly decreased.

III. Pb REGION

We have promised to briefly consider the $A=208$ region of the Periodic Table. The procedures discussed in the earlier sections of this paper were used to determine what were essentially four independent wells for the neutron and proton particle and hole states. The energy shift between the Pb^{209} particle states and their analogs in Bi^{209} played a major role in determining the size of the neutron well. We placed an additional restriction on the proton well, asking that the proton matter distribution, obtained by taking our local well seriously, not possess an rms radius less than that determined in electron scattering. For Pb^{208} the root-mean-square radius we employed was $a_0=5.49$ fm.[21]

The parameters in these wells are displayed in Table VI. Although we did not invoke an independent size parameter for the spin-orbit component, our proton potentials for both particles and holes are not unlike those of Rost.[22] However, our neutron parametrization differs significantly from that of the latter author. We have written the radii for the different Woods-Saxon potentials in the conventional fashion

$$R_0 = r_0 A^{1/3},$$

allowing particle and hole radii to differ only by this explicit mass dependence. Rost[22] has used for his neutron well an r_0 between 1.295 and 1.347 fm, a considerably larger figure than that given in Table VI. Clearly, the Rost well will not correctly describe the analog Coulomb energy shift within our framework for the analog state. In addition there seems to be evidence from stripping data[23] that the Rost well leads to unusually small spectroscopic factors for what one believes to be reasonably good single-particle states

[19] L. Rosenfeld, *Nuclear Forces* (North-Holland Publishing Co., Amsterdam, 1948).
[20] G. E. Brown, Compt. Rend. Congr. Intern. Phys. Nucl. Paris **1**, 129 (1964).
[21] H. L. Acker, G. Backenstoss, C. Daum, J. C. Sens, and S. A. DeWitt, Nucl. Phys. **87**, 1 (1966).
[22] E. Rost, Phys. Letters **26B**, 184 (1968).
[23] G. Igo, E. R. Flynn, P. Barnes, and D. D. Armstrong (to be published).

TABLE VI. Proton and neutron well parameters which are fitted to the proton charge distribution and analog-state Coulomb energy as well as the single-particle and single-hole energies in appropriate nuclei near Pb^{208}. The proton particle and hole wells were identical for all but the $1h_{9/2}$ hole level. To describe the neutron wells, it is convenient to use the oscillator quanta label $\nu=2n+l$. The well parameters listed for the $\nu=7$ level place the $j=15/2^-$ level at the position of the lowest observed level of this character.

	V_0 (MeV)	V_{s0} (MeV)	r_0 (fm)	a (fm)
A. Proton wells level description $(n+1, l, j)$				
$3p_{1/2}, 3p_{3/2}, 2f_{5/2}, 2f_{7/2}, 1i_{13/2}$	60.6	7.40	1.27	0.70
$3s_{1/2}, 2d_{3/2}, 2d_{5/2}, 1g_{7/2}, 1g_{9/2}$	60.6	7.40	1.27	0.70
$1h_{9/2}, 1h_{11/2}$	59.6	11.0	1.27	0.70
B. Neutron holes level description $(2n+l)$				
5	52.0	5.32	1.135	0.70
6	55.0	6.32	1.135	0.70
7	57.8	6.82	1.135	0.70

in Pb^{209}. Smaller neutron valence orbits would increase these spectroscopic factors.[24]

It is of interest to note, parenthetically, that the neutron and photon mass distributions predicted from our local potentials differ in their average radii by only a negligible amount. The neutrons, however, extend well beyond the Coulomb-confined protons. These conclusions had already been arrived at for the Pb isotopes by Nolen *et al.*[25] using a technique which treated the mass distributions in a more direct geometric fashion. With this latter approach, these authors deduce for the neutron excess a rms radius of 5.70 fm, whereas our microscopic picture yields 5.72 fm for this same radius. In Table VII we have listed Coulomb energies and neutron excess radii for ours and a variety of earlier wells.

From the well parametrizations listed in Table VI we see that the neutron particle and hole states cannot be described by the same well depths. To properly bind the particle states one must increase the central and spin-orbit strengths of the well used for holes by 3 and 1 MeV, respectively. This is perhaps equivalent to introducing an effective mass into the particle single-particle Hamiltonian.[26] In this latter discussion we find it necessary to place the $i_{13/2}$ hole state in the particle well. If the hole parameters are used for this level, insufficient binding results. A further deepening of the well is required to place the $j_{15/2}$ single-particle strength at 1.41 MeV above the Pb^{209} ground state (where the first such level is observed). Recent experiments by Igo *et al.*[23] indicate the lowest $15/2^-$ level contains perhaps only 50% of the total single-particle strength. Assuming that the remainder of this strength is located at 3.56 MeV, as suggested by these authors, one still finds it necessary to use a deeper well for the $15/2^-$ state than for the other particle states.

Whether or not the above correlation between oscillator major shell and neutron well depth is significant, one may still conclude that the single-particle wells in the $A\sim208$ nuclei are unusual. The use of different proton and neutron nuclear wells appears to imply that isobaric spin invariance fails for the single-particle part of the nuclear Hamiltonian. If this invariance is to be restored, one must presumably employ a noninvariant residual interaction. We should note at this point that we advocate, at the very least, an isotopic dependence in the proton well. In the analog state where the proton interacts with the neutron excess via only the $T=1$ part of the particle-particle force we use a proton well identical to that for neutrons. In the states of lower isotopic spin, for nuclei with one proton

TABLE VII. Coulomb energies and neutron excess rms radii for our well, Rost's NOT well,[a] and the Blomqvist-Wahlborn well. The Rost (Blomqvist-Wahlborn) well parameters are $V_0=40.5$ (44.0) MeV, $V_{s0}=8.30$ (7.82) MeV, $r_0=1.349$ (1.27) fm, and $a=0.70$ (0.67) fm.

Neutron well	Direct Coulomb energy (MeV)	Neutron excess radius (fm)
Rost[a]	18.16	6.53
Blomqvist-Wahlborn[b]	18.73	6.21
Ours	19.62	5.72
Geometric description of Nolen, Schiffer *et al.*[c]	19.69	5.70

[a] See Ref. 21.
[b] J. Blomqvist and S. Wahlborn, Arkiv Fysik **16**, 545 (1960).
[c] See Ref. 24.

[24] S. A. A. Zaidi and S. Darmodjo, Phys. Rev. Letters **19**, 1446 (1967). These authors have also used a neutron well with a small radius, a well which leads to reasonable spectroscopic factors (Ref. 23).
[25] J. A. Nolen, Jr., J. P. Schiffer, and N. Williams, Phys. Letters **27B**, 1 (1968).
[26] G. E. Brown, J. G. Gunn, and P. Gould, Nucl. Phys. **46**, 598 (1963); G. F. Bertsch and T. T. S. Kuo, *ibid.* **A112**, 204 (1968).

TABLE VIII. Single-particle and single-hole energy for Pb^{208}. The binding energies calculated from the potential wells parametrized in Table VI are compared to the experimental energies. Also listed are (a) the values of $(\hbar\omega)_{max}$ which yield a maximum overlap for each WS wave function with its largest oscillator component and (b) the amplitude a_{max} of this oscillator component when the choice $\hbar\omega=(\hbar\omega)_{max}$ is made in the expansion.

Level	Experimental[a] binding energy (MeV)	Calculated energy (MeV)	$(\hbar\omega)_{max}$ (MeV)	a_{max} (fm)
	(a) Proton particles (Bi^{209})			
$3p_{1/2}$	0.18	−0.14	6.69	0.979
$3p_{3/2}$	−0.57	−0.21	6.50	0.977
$2f_{5/2}$	−0.94	−0.84	7.00	0.985
$1i_{13/2}$	−2.16	−1.92	7.50	0.995
$2f_{7/2}$	−2.87	−2.93	6.62	0.980
$1h_{9/2}$	−3.77	−3.93	7.75	0.996
	(b) Proton holes Tl^{207}			
$3s_{1/2}$	−8.03	−7.71	6.12	0.966
$2d_{3/2}$	−8.38	−8.52	6.38	0.975
$1h_{11/2}$	−9.37	−9.58	7.00	0.993
$2d_{5/2}$	−9.70	−9.84	6.19	0.971
$1g_{7/2}$	−11.51(?)	−12.3	7.06	0.994
	(c) Neutron particles Pb^{209}			
$3d_{3/2}$	−1.42	−1.34	7.81	0.956
$2g_{7/2}$	−1.45	−1.37	8.44	0.988
$4s_{1/2}$	−1.91	−1.98	7.56	0.946
$3d_{5/2}$	−2.36	−2.52	7.81	0.976
$1j_{15/2}$	−2.53	−2.54	9.38	0.998
$1i_{11/2}$	−3.15	−3.39	9.38	0.998
$2g_{9/2}$	−3.94	−4.24	8.25	0.995
	(d) Neutron holes (Pb^{207})			
$3p_{1/2}$	−7.38	−7.22	7.75	0.992
$2f_{5/2}$	−7.95	−7.97	8.12	0.996
$3p_{3/2}$	−8.27	−7.94	7.75	0.992
$1i_{13/2}$	−9.01	−8.76	9.00	0.998
$2f_{7/2}$	−9.72	−9.87	8.00	0.994
$1h_{9/2}$	−10.85	−10.70	8.81	0.998

[a] See Ref. 27.

particle plus a neutron excess composed of closed shells, the proton interacts with the neutron excess through the $T=0$ part of the force. It is this altered environment, for what we have previously referred to as proton particles, that presumably results in a proton well altered in depth and size from the neutron-hole well. The increase in proton well size is reasonable in view of a tendency for protons and neutrons to remain spatially together.

A more consistent treatment would, no doubt, be obtained if one mentally stripped off the neutron excess and considered the entire proton-neutron-excess interactions in detail. However, since it is our intent to follow the usual shell-model procedures for nuclei such as Pb^{206} and Pb^{210} we have submerged the proton-neutron excess interaction into an over-all single-particle potential. This potential was, nevertheless, chosen so as not to violate certain physical features of these nuclei.

Finally, we should, of course, reemphasize that the analog-state Coulomb energies are obtained in the manner discussed in Sec. II for the $A=17$ nuclei. Of course, the relationship between a single-particle state in Pb^{209} and its analog in Bi^{209} is considerably more complex than the relation between the ground states of O^{17} and F^{17}. The entire neutron excess is involved in a characteristic fashion in the heavier nuclei,[27] and in fact the single-particle $g_{9/2}$ component is only a very small part of the total analog wave function. Since this is true also for any of the single-particle excited states, the Coulomb shifts one observes should, to a high degree of accuracy, be state-independent.

In our calculations we chose to fit the Coulomb shift in the Pb^{208}-Bi^{208} pair. We increased the experimentally observed shift of 18.98 MeV by some 0.7 MeV to account for a Coulomb exchange energy. The latter had been estimated by Nolan *et al.*[25] to be 3.5% of the direct Coulomb energy. In the $A=17$ nuclei we omitted reference to an exchange energy; including it would have slightly decreased the effects we obtained. One might also question the accuracy of the form shown in Eq. (10) for the proton-nucleus Coulomb potential. We did not feel that the differences produced by employing, say, a Fermi charge distribution would significantly alter our results.

We have presented, in Table VIII and Fig. 3, the level positions determined from our well and for comparison the experimentally observed energies. Also

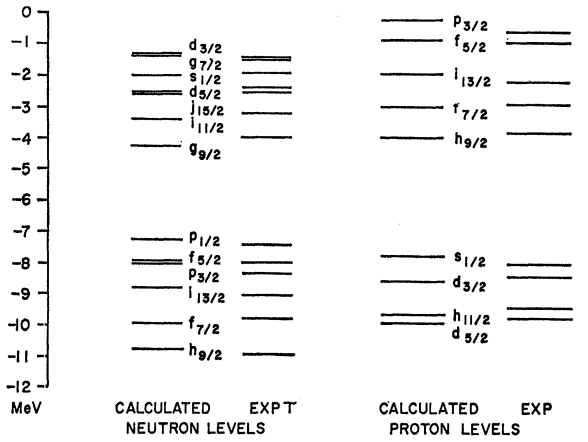

FIG. 3. Diagramatic representation of the fits to single-particle energies in the Pb^{208} region with the potential well of Table VI.

[27] D. Robson, Ann. Rev. Nucl. Sci. **16**, 119 (1966).

presented in Table VIII are the values of the oscillator parameter which leads to a maximum overlap between a WS wave function and its main oscillator component. Clearly, all hole levels and many-particle levels are well described by a single-oscillator component. Typically particle states with low angular momentum and several nodes require a multicomponent oscillator description. In any case, no single value of the oscillator parameter can be used to give an adequate single-oscillator function representation of all levels. In particular there is a considerable disparity between what one might regard as an average proton value $\hbar\omega=6.75$ MeV and an average neutron value $\hbar\omega=8$–9 MeV. A structure calculation involving both neutron and proton levels is then no longer simple. Even if one employs a single-oscillator component for protons and neutrons separately to calculate interaction matrix elements, one will be forced to expand one or other of the sets of wave functions in the mode of Eq. (2).

For our illustrative calculations in the Pb region we have employed as a residual interaction the separable-potential-based free-reaction matrix $K(\epsilon)$ for the choice $\epsilon=-200$ MeV. Although a proper nuclear reaction matrix calculation should be performed to determine the bare residual interaction, we felt the above choice would be adequate for delineating the effect of WS wave functions. It should be noted that our bare force does not take account of the asymmetric treatment of the Pauli principle in intermediate states that is required in the presence of a neutron excess. The latter may have serious consequences for the residual interaction.

In Table IX we display spectra for Pb^{206} and Pb^{210} obtained from a WS calculation and from pure oscillator calculations for $\hbar\omega=6$ MeV and 8 MeV. For comparative purposes, both the unperturbed and experimental positions of levels are included. It is immediately evident that the valence particle-particle or hole-hole interactions for the Pb isotopes are considerably weaker than those observed in light nuclei. With the exception of the ground-state energies for the two nuclei considered in Table IX, most levels suffer shifts due to the interaction which are small relative to the unperturbed spacings between configurations. In most cases the changes produced by employing WS wave functions are also small and seem inconsequential in relation to other uncertainties in level position and structure.

The hole states for a single type of particle are, as we have indicated, rather well described by single oscillator functions. One does not therefore expect WS functions to alter calculated hole spectra, provided of course one employs the correct value of $\hbar\omega$. In particular, we see that the interaction energy for the ground state of Pb^{206} predicted by a WS calculation is bracketed by the energies obtained from oscillator calculations. In contrast, the corresponding WS energy for the ground state of Pb^{210} is less than the value obtained with either

TABLE IX. (a) Pb^{206} and (b) Pb^{210} spectra obtained from WS calculations and from oscillator calculations with $\hbar\omega=6$ and 8 MeV. The fundamental free-reaction matrix with $\epsilon=-200$ MeV is used as a residual interaction. The unperturbed and experimental level positions are listed for comparison. Only a few states were considered in the WS diagonalizations because of the large amounts of computer time required. For Pb^{206} one can probably trust the oscillator calculations for $\hbar\omega=8.0$ MeV. All energies are in MeV.

J^π	Unperturbed	Experiment[a]	Oscillator $\hbar\omega=6.0$	Oscillator $\hbar\omega=8.0$	WS
		(a) Pb^{206}			
0^+	0.00	−0.64	−0.37	−0.52	−0.46
	1.14	0.52	0.62	0.58	0.60
1^+	0.89	1.09	0.84	0.83	0.81
	1.46	(1.51)	1.40	2.82	1.39
2^+	0.57	0.16	0.24	0.00	0.08
	0.89	0.82	0.59	0.54	0.48
	1.14	1.14	1.03	0.99	1.00
3^+	0.57	0.70	0.54	0.52	0.53
	1.46	2.48	1.39	1.34	1.34
4^+	1.14	1.04	1.05	0.93	
	1.46	1.36	1.22	1.16	
	2.20	2.28	2.21	2.18	
5^+	2.91		2.84	2.80	
	3.26		3.18	3.16	
6^+	2.91	(2.61)	2.48	2.29	
	3.26		3.18	3.16	
3^-	3.97	1.89	3.69	3.63	3.66
4^-	2.20		2.14	2.11	2.11
	3.97		3.90	3.84	3.82
5^-	2.20	2.14	2.13	2.09	2.12
	3.97	(2.55)	2.37	2.33	2.34
6^-	1.63	1.74	1.60	1.58	
	2.20		2.16	2.14	
7^-	1.63	1.56	1.50	1.44	
	2.20		2.12	2.10	
8^-	2.20		2.16	2.13	
	2.52		2.49	2.48	
9^-	2.20	(2.01)	1.95	1.84	
	3.97		3.93	3.92	
10^-	3.97		3.94	3.93	
		(b) Pb^{210}			
0^+	0.00	−1.24	−0.68	−0.76	−0.55
	1.58		0.91	0.90	0.98
1^+	0.79		0.68	0.66	0.72
	2.49		2.41	2.42	2.36
2^+	0.00	−0.44	−0.24	−0.34	−0.30
	0.79		0.77	0.74	0.79
4^+	0.00	−0.15	−0.11	−0.15	
6^+	0.00	−0.05	−0.06	−0.09	
8^+	0.00	+0.03	−0.04	−0.06	
2^-	2.20		2.03	2.00	2.00
3^-	1.41		1.17	1.14	1.16
	2.20		2.10	2.04	2.03
4^-	1.14		1.32	1.25	1.22
	2.20		2.09	2.05	2.05

[a] W. W. True, Phys. Rev. **168**, 1388 (1968).
[b] C. Reidel, R. A. Broglia, and A. Miranda, Nucl. Phys. **A113**, 503 (1968).

$\hbar\omega=6$ or 8 MeV. The particle-particle states expected to be most affected by the use of WS functions unfortunately lie higher up, in energy regions as yet unexplored experimentally.

Since the radii of the Pb nuclei are considerably larger than the range of the bare force, one might have expected the $\hbar\omega$ dependence of our potential to be described simply in terms of geometry. If only the relative s-wave part of the force were included one would in fact observe a proportionate increase in the size of oscillator matrix elements as $\hbar\omega$ increased. However, the triplet-odd part of the potential, in particular the relative $^3P_1$ state, seems to be strong and repulsive in its contribution to the residual interaction. The combined interaction from the $^1S_0$, $^1D_2$, and $^3P_1$ states is then much less sensitive to $\hbar\omega$. Indeed in certain cases increasing $\hbar\omega$ can lead to a decrease in attractive matrix elements, and even repulsive matrix elements may result if the singlet-even potential is overwhelmed.

Table IX lists the $J=0^+$ matrix elements appropriate to Pb^{210} for a variety of situations. The eventual outcome in Pb^{210} we recall was, as one might have expected, an increase in the binding energy of the lowest 0^+ level when $\hbar\omega$ was increased from 6.0 to 8.0 MeV. This increase was, however, less than a purely geometric argument would have yielded. For particle-particle or hole-hole states coupled to higher total angular momentum, the role of the $^3P_1$ state diminishes and one will for such states find more sensitivity to $\hbar\omega$.

Our spectra for Pb^{206} and Pb^{210} are not likely to be good fits to the experimentally observed levels. We have employed only the bare force, neglecting for the moment core polarization. Kuo[28] has found, using a bare force also calculated in an approximation ignoring the neutron excess, that on occasion the core polarization contribution is considerably larger than the bare interaction. Such corrections may, for example, yield the additional binding energy required in the ground states of Pb^{206} and Pb^{210}.

[28] T. T. S. Kuo (report of work prior to publication) and (private communication).

Kuo[28] has, in his study, considered the particle-hole states of Bi^{208}. Of particular interest is the separation between the Pb^{208} analog state and the low-lying particle-hole states of one unit less in isotopic spin. Kuo's calculation,[28] which employs a common oscillator field with $\hbar\omega=7$ MeV for the proton in the analog state or in the low-lying states and the same field for the neutron holes, appears to underestimate this energy. We have suggested using different nuclear wells for the proton particles in the two types of states, and in addition prefer a considerably larger $\hbar\omega$ value close to 9 MeV, for some of the important constituents of the analogue state. Indeed if for the O^+ states of Bi^{208} the particle-hole interaction were as weak as we have observed the hole-hole and particle-particle interactions to be, then the energy separation we have been referring to is already present in the single-particle symmetry energy of the nuclear average fields. Of course, in principle, one ought also to predict this symmetry energy from the interaction of a proton with the neutron excess. At this point the bare force may prove inadequate.

We would like, finally, to comment on what appears to be a possible inconsistency in our approach. First the realistic interactions we use have not contained any core-mediated force[2]; that is, they have been bare residual interactions. Just how matrix elements of this quite significant part of the force are altered by WS single-particle wave functions, we cannot say without further calculation. Secondly, and perhaps more disturbing, our bare force has been obtained from a reaction matrix calculation which invoked either an oscillator or plane-wave basis for intermediate states. One might speculate that sizeable changes in the bare interaction would result from the use of WS functions for the intermediate states. However, since one sums over an essentially complete set of intermediate states, such an eventuality is unlikely.

The calculations in this work were done on the CDC-6600 Computer at the Brookhaven National Laboratory Computing Center.